The mouse lymph node as an ectopic transplantation site for multiple tissues

Junji Komori[1,*], **Lindsey Boone**[1,*], **Aaron DeWard**[1,*], **Toshitaka Hoppo**[1,2], and **Eric Lagasse**[1]

[1]McGowan Institute for Regenerative Medicine, Department of Pathology, University of Pittsburgh School of Medicine, Pittsburgh PA

Abstract

Cell-based therapy has been viewed as a promising alternative to organ transplantation, but cell transplantation aimed at organ repair is not always possible. Here, we show that the mouse lymph node can support the engraftment and growth of healthy cells from multiple tissues. Direct injection of hepatocytes into a single mouse lymph node generated enough ectopic liver mass to rescue survival of mice with lethal metabolic disease. Furthermore, thymuses transplanted into a lymph node of athymic nude mice generate a functional immune system capable of rejecting allogeneic and xenogeneic grafts. Finally, pancreatic islets injected into the lymph node of diabetic mice restore normal glucose control. Collectively, these results suggest the practical approach of targeting lymph nodes to restore, maintain or improve tissue and organ functions.

Introduction

The shortage of organs available for transplant to terminally ill patients represents a major worldwide medical, social, and economic challenge. An alternative approach to whole-organ transplant involves the transplantation of cells to regenerate failing organs[1,2]. However orthotopic cell-based therapy directed at a diseased organ may not be feasible for many reasons, ranging from a possible lack of an appropriate environment in cirrhotic and fibrotic liver during end-stage disease to the lack of a thymus in complete DiGeorge Syndrome[3–5]. Consequently, a critical requirement of cell-based therapy for these patients is to establish an optimal *in vivo* site for cell and tissue transplantation to restore organ functions[6,7].

The lymph node (LN) is a key organ of the mammalian immune system that has evolved to mount an immediate and orchestrated response against invading pathogens. The LN acts as a checkpoint where migrating T and B cells may encounter foreign antigen[8,9]. If a foreign

Correspondence: Eric Lagasse, PharmD, PhD., McGowan Institute for Regenerative Medicine, University of Pittsburgh, 450 Technology Drive. Room: 329, Pittsburgh, PA 15219, Phone: 412-624 5285, Fax: 412-624-5363, Lagasse@pitt.edu.
*These authors contributed equally to this work
[2]Current address, Department of Surgery, West Penn Allegheny Health System, Pittsburgh PA.

antigen is identified, T cells undergo rapid cell division and also signal for help and recruit additional T cells[8,9]. To accommodate this sudden increase in cell number, lymphocytes need a special environment, which the LN provides.

Interestingly, the LN is also one of the first clinically observed sites of most cancer metastasis. Selected cancer cells will often migrate away from a primary tumor and colonize the LN[10]. Lymphatic vessels are designed to facilitate the uptake of surrounding fluid and cells, followed by transport of this fluid and cells to a nearby LN[10]. Therefore, malignant tumor cells take advantage of this route normally traveled by immune cells. Upon arrival in the LN, tumor cells can survive, perhaps because the architecture of the LN provides direct access to essential nutrients and growth factors found in the blood through the high endothelial venules. The LN also contains fibroblastic reticular cells and other stromal cells that secrete chemokines to enhance cell recruitment and survival[8,9,11].

Because LNs support normal immune function as well as survival of metastatic tumor cells, LNs might also promote survival and expansion of healthy cells and tissues. Healthy cell and tissue growth in LNs would provide a new approach for cell therapies in regenerative medicine.

Here, we test the hypothesis that when transplanted directly into the LN of mice, three distinct healthy cell types would engraft and demonstrate ectopic organ functions *in vivo*. Previously, our lab showed that primary hepatocytes injected intraperitoneally into mice lacking fumarylacetoacetate hydrolase, (a mouse model of tyrosinemia type I) migrate and colonize the host abdominal lymphatics and restore hepatic functions[13]. Here, we show that hepatocytes injected directly into a single jejunal, popliteal, axillary, or periportal LN generate an ectopic hepatic mass and rescue mice from lethal liver failure. Furthermore, thymic tissue injected into a single jejunal LN of athymic nude mice generates a functional ectopic thymus. Finally, pancreatic islets transplanted in a single jejunal LN of streptozotocin induced diabetic mice engraft and secrete insulin to normalize glucose levels. These three independent results support the proof-of-concept that the LN provides a hospitable environment for normal cell engraftment and reveal a new approach to consider for future ectopic tissue and organ regeneration.

Results

Direct injection of hepatocytes into the LN

We targeted a single jejunal LN in the abdominal cavity of C57BL/6 wild type mice, which was selected because it is easily accessible and relatively large[14]. Upon injection of 0.1–0.5 million syngeneic primary hepatocytes, the LN enlarged slightly and no visible leakage was found, as evidenced by Evans blue dye (Fig. 1a). One day after injection, syngeneic luciferase-expressing hepatocytes remained in the LN, as determined by *in vivo* imaging of luciferase (Fig. 1b). In contrast, splenic and intraperitoneal injection of hepatocytes resulted in rapid dispersion of cells to the liver and throughout the abdominal cavity, respectively (Fig. 1b). One week after transplant, syngeneic GFP+ hepatocytes were distributed mainly in the subcapsular sinus of the LN, but were not found in the LN follicle or germinal center (Fig. 1c). Additionally, hepatocytes rapidly formed patches of hepatic tissue expressing E-

cadherin (Fig. 1d). This hepatocyte-to-hepatocyte attachment may help to retain hepatocytes within the site of transplantation[15]. Furthermore, the cell trafficking molecule sphingosine-1-phosphate receptor 1 (S1PR1), which is necessary for the egress of B and T cells from LNs [16,17], was not present on hepatocytes in the LN. On the other hand, CCR7, a molecule known to control the migration of memory T cells and/or tumor cells into LNs [18], was expressed by hepatocytes in the LN (Fig. 1d). These observations suggest a potential mechanism of retention of healthy hepatocytes in the LN.

To assess whether the engrafted hepatocytes in the LN proliferate in response to growth stimuli in C57BL/6 wild type recipient mice, we performed partial hepatectomy (PHx) one week after syngeneic hepatocyte injection into the LN and added bromodeoxyuridine (BrdU) to the drinking water of recipient mice. PHx is a physiologically relevant method of stimulating hepatocyte growth[19]. BrdU incorporation was analyzed in the LN engrafted hepatocytes 2 weeks after LN injection and compared with animals that were not subjected to PHx. The number of GFP-expressing hepatocytes and percent of BrdU$^+$ hepatocytes in the LN of the PHx group was significantly higher than in mice without PHx (Fig. 1e), indicating that hepatocytes in the LN respond to growth stimuli after PHx.

A functional ectopic liver in the LN

Next, we asked whether transplantation of syngeneic hepatocytes into a single jejunal LN of Fah$^{-/-}$ tyrosinemic mouse[20–22], a model of lethal metabolic liver failure, would induce hepatocyte proliferation. Twelve weeks after hepatocyte injection into the LN, animals were rescued from lethal liver failure due to the newly hepatized growth in the jejunal LN (Fig. 2). Hepatocyte engraftment was localized to the transplanted LN and was not observed in other LNs or in the native liver (Fig. 2a), suggesting that lymphatic distribution of hepatocytes did not occur. The 'hepatized' LN was mostly composed of newly formed liver tissue containing Fah$^+$GFP$^+$ hepatocytes, but also included remnants of the lymphatic system as revealed by surrounding LYVE1$^+$ lymphatic endothelial cells (Fig. 2b). The LN was transformed into a hepatic organoid composed of characteristically cuboidal hepatocytes, but with the absence of a biliary system[13]. To define the hepatized LN microarchitecture, we stained recipient LN for ER-TR7, a marker of fibroblastic reticular cells (FRCs), dipeptidyl peptidase-4 (DPP IV), a marker for brush borders of hepatocytes and bile canaliculi organization, and glutamine synthetase (GS), a marker of zonality for hepatocytes surrounding the terminal hepatic venules[23] (Fig. 2b). GFP$^+$ hepatocytes resided in cellular proximity with ER-TR7$^+$ FRCs. FRCs are known to play a crucial role in establishing the reticular network as well as regulating immune function[11,24]. Similar to what is observed in normal liver anatomy, DPP IV was localized throughout the hepatized LN. Moreover, GS$^+$ hepatocytes were identified surrounding some of the hepatic veins in the newly formed liver tissue. Notably, we observed survival of the animals (Fig. 2c) and long-term persistence (over 25 weeks) of the graft after transplantation to the LN (Fig. 2a) and no immune-responsiveness as indicated by the presence of very few lymphocytes and macrophages around the transplantation zone (Supplementary Fig. 1).

We then tested if this transplantation method is effective in other LNs throughout the body, since all LNs share a common histological architecture[9,14,25]. We injected syngeneic

hepatocytes into single extra-abdominal axillary or popliteal LNs in Fah$^{-/-}$mice (Fig. 2a). Similar to the intra-abdominal jejunal LN injection, we observed a single, large, hepatized LN several weeks after cell transplantation, which subsequently rescued mice from lethal liver failure (Fig. 2c). In wild type mice, a jejunal LN weighs around 25±3 mg whereas a popliteal or axillary LN weighs 3±1 mg (n=5). Because the jejunal LN is the largest LN in the mouse, it was consequently easier to inject and lead to a higher survival rate (Fig. 2c). Furthermore, when we compared the mass of hepatic tissue generated in the intra-abdominal jejunal LN to the extra-abdominal axillary and popliteal LNs, we found no statistical differences, indicating no tissue growth advantage between these 3 LNs (Fig. 2d). Transplantation of hepatocytes into a periportal LN, one of the closest LNs to the liver, also resulted in a large hepatized LN and rescued the mice from lethal liver disease. However, transplantation of a LN closer to the location of the liver did not appear to be beneficial for the experimental outcome when compared with the other transplanted LNs (Fig. 2d).

Thus far all transplantations used syngeneic donor and recipient mice. Because LNs perform a central function for allogeneic recognition[26], we next tested whether successful engraftment is possible in allogeneic LN. We injected C57BL/6-GFP$^+$ hepatocytes into the liver (via splenic injection) or into the LN of 129sv FAH$^{-/-}$ recipient mice. 129sv and C57BL/6 mice share the major histocompatibility complex haplotype H2^b but differ in minor histocompatibility antigens and are considered allogeneic[27,28]. While C57BL/6 hepatocytes transplanted into 129sv FAH$^{-/-}$ recipients failed to engraft (Fig. 2e), blocking the co-stimulation pathways CD28/B7 (blocked by CTLA4Ig) and CD40/CD40L (blocked by MR1)[29,30] in the 129sv FAH$^{-/-}$ recipients facilitated successful engraftment of C57BL/6-GFP$^+$ hepatocytes injected into either the spleen or the LN (Fig. 2e). This result shows that the immune reaction to transplanted cells in LNs is not stronger or faster compared to cells transplanted in another site.

A functional ectopic thymus in the LN

Using a similar approach, we asked if *de novo* thymus function could be generated in LNs of athymic mice. Thymuses were harvested from newborn C57BL/6 GFP$^+$ transgenic mice, minced and injected directly into the jejunal LN or under the kidney capsule of athymic BALB/c Nude mice. After one month, recipient mouse blood was analyzed by flow cytometry for the presence of recipient (GFP) single positive (SP) CD4$^+$ and CD8$^+$ T cells. Thymic transplant into the LN (LN Tx Nude) or under the kidney capsule (KC Tx Nude) generated circulating recipient SP CD4$^+$ and CD8$^+$ T cells (Fig. 3a, Supplementary Fig. 2). Ten months after transplantation, SP CD4$^+$ and CD8$^+$ T cells were still present in the peripheral blood indicating long-term thymic engraftment in the LN (Supplementary Fig. 3). Interestingly, transplantation of a thymic single cell suspension also resulted in the presence of SP CD4$^+$ and CD8$^+$ T cells, although to a lesser degree than transplantation of minced thymic tissues (Supplementary Table 1). Newborn GFP$^+$ mice were used as a source of donor thymuses because they contain minimal mature thymocytes. In fact, less than 6% (n=3/54) of recipient mice showed any donor GFP$^+$ T cell contamination in the blood one month after transplant, when measured by flow cytometry (data not shown). These three mice were excluded from further studies.

We then harvested the ectopic thymuses for further characterization of the engraftment. GFP[+] epithelial thymic cells remained within the injected LN and were organized into an epithelial thymic structure (Fig. 3b). Previously, thymic epithelia have been distinguished by their cytokeratin 5 (K5) and cytokeratin 8 (K8) phenotypes[31]. The ectopic thymuses were present in the subcapsular sinus of the LN (Supplementary Fig. 4) and contained both K5 and K8 positive regions, which correspond with thymic medullary and cortical epithelia, respectively (Fig. 3b). Ectopic thymuses were also analyzed for the presence of recipient double positive (DP) CD4^{+}CD8^{+} thymocytes, which represent immature T cells undergoing thymic selection[32]. The ectopic thymuses contained recipient DP thymocytes as well as SP CD4^{+} and CD8^{+} T cells, indicating a selective mechanism of T cell commitment and maturation (Fig. 3b).

To more fully characterize the T cell phenotypes generated in the LN Tx Nude mice, we analyzed the T cell receptor (TCR) repertoire by flow cytometry staining with antibodies recognizing different TCR Vβ segments (Vβ 2, 3, 4, 5.1–5.2, 6, 7, 8.1–8.2, 8.3, 9, 10[b], 11, 12, 13, 14, and 17[a]). Each Vβ was detected on CD3^{+} T cells of C57BL/6 wild type splenocytes. Heterozygous BALB/c Nude mouse splenocytes expressed 10 out of 15 Vβ segments, consistent with known partial or complete genetic deletions of certain Vβ segments (Vβ 3, 5.1–5.2, 9, 11 and 12) in this strain. Importantly, splenocytes in LN Tx Nude recipients expressed a Vβ profile similar to the heterozygous BALB/c Nude mice (Fig. 3c). These results demonstrate that a C57BL/6 ectopic thymus promotes development of T cells generated from the bone marrow of recipient BALB/c Nude mice.

We then further characterized the splenic T cells in LN Tx Nude mice by flow cytometry to determine whether regulatory, naïve, central memory, and effector memory T cell subsets are present. Regulatory T cells were detected by analyzing FoxP3 expression in CD4^{+}CD25^{+} T cells. We observed similar percentages of regulatory T cells in splenocytes from C57BL/6, heterozygous Nude, and LN Tx Nude mice (Fig. 3d). Naïve and memory T cells were distinguished by the differential expression of CD44 and CD62L (naïve: CD44^{−}CD62L^{+}, central memory: CD44^{+}CD62L^{+}, and effector memory: CD44^{+}CD62L^{−}). As with the regulatory T cells, we detected naïve and memory T cell subsets among splenocytes from C57BL/6, heterozygous Nude, and LN Tx Nude mice (Fig. 3d). The percentage of effector memory T cells was higher and naïve T cells was lower in the LN Tx Nude mice, perhaps because these mice had been previously exposed to skin grafts (see below).

Since LN Tx Nude mice contained a range of peripheral SP CD4 and CD8 T cells, we asked if the *de novo* immune system in these recipient mice could mount a T cell-mediated response against a skin allograft. Tail skin from C57BL/6 (syngeneic with regard to the donor thymus) or CBA/CaJ (allogeneic with regard to the donor thymus) mice was transplanted to the dorsal side of LN Tx BALB/c Nude mice. After 2 weeks, all of the LN Tx BALB/c Nude mice had rejected the allogeneic CBA/CaJ skin grafts. On the other hand, the C57BL/6 skin grafts were completely accepted after 2 weeks (Fig. 3e). We then asked if LN Tx BALB/c Nude mice would also mount an immune response against a xenogeneic tumor cell transplant. 300,000 human colorectal cancer cells[33] were injected into the subcutaneous space of BALB/c Nude and LN Tx BALB/c Nude mice. The majority (8 of 9)

of injected LN Tx BALB/c Nude mice rejected the tumors (Fig. 3e). In contrast, xenogeneic tumors grew in untreated BALB/c Nude mice (Fig. 3e). These results suggest that the SP T cells present in LN Tx BALB/c Nude mice were functional. Together, these data support the concept of using the LN as a site for thymic transplant to generate an ectopic thymus.

Functional pancreatic islets in the LN

Finally, we hypothesized that the LN would also provide a suitable environment for pancreatic islet transplantation. Islets were harvested from C57BL/6 GFP[+] transgenic mice and transplanted into the jejunal LN of C57BL/6 wild type mice treated with streptozotocin, which induces diabetes. Blood glucose levels were monitored weekly and the transplanted LN was eventually removed to analyze islet engraftment.

GFP[+] islets were found within the subcapsular sinus of the LN, adjacent to the densely packed lymphocytes indicative of a typical LN (Fig. 4a). We detected expression of C-peptide and glucagon, markers of pancreatic β-cell and α-cell function, respectively, within the engrafted LN (Fig. 4a).

Next, we asked whether islets transplanted to the LN of diabetic mice (blood glucose levels greater than 300 mg/dL) are able to lower blood glucose levels to a normal range (blood glucose levels between 100–200 mg/dL). Similar to islets transplanted under the kidney capsule, islets transplanted directly into the LN restored mean blood glucose levels to normal levels within six weeks after transplantation (Fig. 4b). In 3 of 5 LN Tx mice, a second islet transplant was performed into the jejunal LN one week after the initial transplant. Furthermore, normoglycemia was maintained in the one mouse examined at six months for at least six months after LN transplantation (data not shown). These results suggest that pancreatic islets transplanted in the LN survive and function *in vivo* with the capacity to sustain long-term normoglycemia.

Because we observed engraftment of multiple cell types in the LN, we asked whether activation of a LN-mediated immune response might interfere with the function of the engrafted cells. Therefore, we induced an inflammatory reaction in the intraperitoneal cavity of normoglycemic mice that had received islet transplants into their LN; to induce the inflammatory reaction we injected mice with lipopolysaccharide (LPS, 1 mg/kg). We confirmed the effective induction of inflammation by measuring the serum levels of tumor necrosis factor α (TNF α), interleukin 1β (IL-1β), and IL-6 (Fig. 4c). Immediately after LPS injection, we noted a temporary reduction in mouse weight and blood glucose levels, which completely normalized after four days (Fig. 4c). We did not observe any increase in glucose levels above normal levels (normoglycemia was still detected 5 weeks after LPS injection). Together, these data suggest no apparent negative effect of the lymphatic or immune systems on LN-grafted islets.

Vasculature of injected LN

We demonstrated that cell engraftment in the LN is not restricted to one cell type. This result is consistent with the current concept of metastasis to the LN, where multiple cancer cell types are capable of residing, and suggests that the LN environment is exceptionally well

suited to promote survival and function of transplanted cells in general. Because abundant vasculature is required to sustain organ function[6,34], we hypothesize that the dense vascular network in the LN is an important contributor to sustain long-term engraftment of normal epithelial tissue. We observed dense neovascular trees in the LNs into which hepatocytes had been injected (Fig. 5a). LN injected with hepatocytes, thymic cells or islets contained many recipient derived CD31^{+} endothelial cells pervading the areas of engraftment, suggesting that extensive blood vessel remodeling took place during ectopic tissue engraftment (Fig. 5b **and** Supplementary Fig. 5). Moreover, we detected CD105^{+} (Endoglin) cells and Collagen IV^{+} cells, which are markers of neovascular remodeling, in each of the engrafted LNs (Fig. 5b)[35–37]. These data suggest that blood vessels in the surrounding LN environment contribute to the neovascularization and overall function of the ectopic tissues.

Discussion

There are over 500 LNs in the human body, many of which are relatively easily accessible. While a single LN structurally limits the number of donor cells that can be transplanted, it is technically feasible to transplant more than one LN in order to gain sufficient organ/tissue function from the transplanted cells. The potential loss of function in a few LNs does not appear to compromise the overall function of the lymphatic system. In fact, lymphedema is the most common complication following lymphadenectomy in patients with cancer and only affects a limited number of patients[38]. Compression syndrome and lymphatic spread are two of the common issues found in cancer patients with metastatic diseases in their LNs. However, none of these complications were observed in any of our experiments. It is also important to note that we transplanted healthy, not transformed, cells into LNs, so the intrinsic potential of transformed cells for widespread metastatic migration and uncontrolled growth is not present in our experiments. Large animal studies will provide further insight into potential difficulties associated with cell transplant to the LN.

LN biopsies by fine-needle aspiration are a routine diagnostic procedure with LNs often being readily identified by palpation or using ultrasound guidance. In fact, the clinical application of LN injection has been validated, with patients rating the procedure as less painful than venous puncture[39]. Moreover, if a less superficial node is advantageous for therapy, ultrasound guidance can be used to successfully inject the visceral mesenteric LNs[40]. The strong clinical precedent of ultrasound-guided LN injections may help make this technique readily adaptable to a clinical setting. These minimally invasive techniques may also allow a potential therapy for patients who are ineligible for a more invasive therapy due to co-morbidities.

In the treatment of liver failure, transplantation of hepatocytes into ectopic sites, including the spleen, pancreas, peritoneal cavity, and subrenal capsule has been proposed. Feasibility and efficacy of these techniques have been confirmed in preclinical studies, but clinical success rates have been limited thus far and new methods are needed to improve hepatocyte engraftment[1,7]. It should be noted that our goal is not to replace a whole liver but to complement liver functions by generating functional ectopic hepatic tissue. In the Fah^{−/−} mice, we generated around 70% of the liver mass in one LN. The native liver is still present, however at a reduced size and probably at reduced function. For patients with liver disease,

we postulate that liver function gradually deteriorates and that transplantation of several LNs with hepatocytes will create enough hepatic mass to stabilize the liver disease. In addition, we hypothesize that hepatic mass generated in the LN may provide enough hepatic function to facilitate regeneration of the native liver. It should also be noted that transplantation of heterotopic liver has been discussed at length in the literature as a possible option to orthotopic liver transplantation [35,41,42].

Thymus transplants have been performed exclusively in the quadriceps of pediatric patients with complete DiGeorge Syndrome[4]. Unfortunately, children with DiGeorge syndrome often show poor growth, and transplantation is frequently postponed to allow for further development[43]. Furthermore, a lack of vascularization and resulting ischemia following transplant is detrimental[44]. Transplanting thymic cells into the LN may represent an advantageous site to provide thymic function.

The optimal implantation site for pancreatic islet transplantation to increase function, reduce necessary implantation mass and decrease immunogenicity is still under debate [6,12,45,46]. But clearly, the proximity to a good vascular supply is essential for survival of islet cells, as well as for hepatocytes and thymic epithelial cells.

One concern for cell transplant into the LN is the rapid immune response that could be initiated by the introduction of foreign antigen into a site densely packed with lymphocytes. In our study, we included experiments under allogeneic conditions and blocked the T cell response to prevent any alloreactivity. We observed that the immune reaction in LNs is not stronger or faster than in other sites and that immune suppression therapy works at similar efficiency compared to the classic hepatocyte transplantation in the spleen. We expect that immunosuppressive therapies similar to those used in clinical organ transplants can be utilized with this approach.

Reprogramming of somatic cells provides an exciting potential source of donor cells for regenerative medicine[47]. Since these cells can be derived from autologous material and are capable of being recognized as "self" by the host immune system, they can potentially overcome immunologic barriers. However, recent studies suggest that these autologous cells may not be entirely protected from the immune system[48]. Based on our results, the LN may provide an effective transplantation site for reprogrammed somatic cells developed for organ regeneration purposes.

In summary, we provide the first report describing the use of a LN as a site for functional cellular transplant. By directly injecting the LN with hepatocytes, thymuses, or pancreatic islets, we demonstrate engraftment of the donor cells and subsequent organ function. This new approach of using the LN as an *in vivo* bioreactor in which to regenerate functional organs may be beneficial to the field of regenerative medicine.

Methods

Animals and tissues

Donor 129sv mice and recipient 129sv Fah$^{-/-}$ mice were a kind gift from Dr. Markus Grompe (OHSU). For allogeneic experiments, donor hepatocytes were isolated from C57BL/6 GFP$^+$ mice (GFP transgene under the control of the human ubiquitin C promoter, C57BL/6-Tg(UBC-GFP)30Scha/J, Jackson Laboratory) and transplanted into 129sv Fah$^{-/-}$ mice. For syngeneic experiments using C57BL/6 GFP$^+$ hepatocytes, 129sv Fah$^{-/-}$ mice were backcrossed for more than eight generations with C57BL/6 mice (Jackson Laboratory) to generate C57BL/6 Fah$^{-/-}$ mice. Luciferase C57BL/6 transgenic mouse (Luc+), expressing firefly luciferase under the control of the broadly expressed beta-actin promoter were kindly provided by Dr. Thorn (University of Pittsburgh). Donor primary hepatocytes were isolated from adult (5–8 weeks old) mice. Donors and recipients were not matched according to gender. Newborn (1–3 day old) C57BL/6 GFP$^+$ mice were used as donors of thymic cells. Athymic BALB/c Nude-*Foxn1^{nu}* (Harlan) mice were used as recipients of thymic cells. Blood collection (100 microliters) was performed using the submandibular bleeding technique. Adult (5–8 weeks old) C57BL/6 GFP$^+$ mice were used as the donor of pancreatic islets. Adult (5–8 weeks old) C57BL/6 mice were used as recipients of pancreatic islets. Animals were bred and housed in the Division of Laboratory Animal Resources facility at the University of Pittsburgh Center for Biotechnology and Bioengineering. Experimental protocols followed National Institutes of Health guidelines for animal care and were approved by the Institutional Animal Care and Use Committee at the University of Pittsburgh.

Hepatocyte Transplantation

Primary hepatocytes were isolated using the 2-step collagenase perfusion technique. The number and viability of cells were determined by trypan blue exclusion. 0.1–0.5 million viable cells were suspended in 20 μl Matrigel (BD Biosciences) for one recipient and kept on ice until transplantation. Recipient animals were anesthetized with 1–3% Isoflurane and laparotomized. The jejunal LN was exposed and cells were injected using a 28 G needle under a dissecting scope (Leica). Just after injection, the contact site was clipped for 5 minutes by micro clamp to prevent cell leakage. In Fah$^{-/-}$ mice experiments, the mice were kept on 2-(2-nitro-4-trifluoromethylbenzoyl)-1,3-cyclohexanedione (NTBC)-containing drinking water at a concentration of 8mg/L until transplantation. NTBC was discontinued just after surgery. For extra-abdominal LN injections, we injected 3% Evans blue solution intradermally into the footpad of the hind or forelimb before cell transplant to visualize the small popliteal or axillary LN.

Thymic Transplantation

Thymuses were harvested from newborn GFP transgenic mice and cut into small fragments. The jejunal LNs were exposed and cells were injected with minced thymus tissue through a 20 G needle. Thymus tissue was also grafted beneath the kidney capsule as a positive control. For the kidney capsule experiments, an incision was made on the left side of the peritoneal cavity and the kidney exposed. A small hole was made in the capsule and the

thymus was inserted between the kidney capsule and parenchyma. Light cauterization was used to seal the opening. The wound was closed with surgical sutures.

Pancreatic Islet Transplantation

Recipient C57BL/6 mice were injected with 190 mg/kg streptozotocin (Sigma) intraperitoneally to induce diabetes. Diabetes (blood glucose greater than 300 mg/dL) was confirmed three days after injection using a Contour Blood Glucose Meter (Bayer). The pancreases from adult C57BL/6 GFP[+] transgenic mice were perfused with Collagenase P (Roche) through the bile duct. Digested islets were washed in HBSS/FBS and placed in a 70 μm cell strainer. The larger size cell strainer content was transferred to a petri dish and individual islets were picked and counted under a dissecting microscope. Approximately 200–300 islets were mixed with 10 ul of matrigel and loaded into a 27 G insulin syringe on ice. For LN transplantation, a small incision was made in the abdomen to expose the jejunal LN. The syringe containing islets was inserted into the LN and islets were slowly injected. For kidney capsule transplantation, a small incision over the left kidney was performed to expose the kidney. A hole was made in the capsule and islets were delivered similar to the LN. Light cauterization was used to seal the opening. The wound was then closed with surgical sutures. If a decrease in glucose level was not observed after one week, a second islet transplant was performed in the same LN.

In vivo Imaging

To detect donor luciferase[+] C57BL/6 hepatocytes, we used an IVIS200 system (Caliper LifeScience) following intraperitoneal injection of 200 μl of 30 mg/mL luciferin substrate into recipient C57BL/6 mice and anesthesia with 3% isoflurane. Images were analyzed using LivingImage software (Caliper LifeScience).

Proliferation Assay

Primary hepatocytes from C57BL/6 GFP[+] mice were transplanted into 11 mice as described above. Recipient mice were given drinking water containing 0.8 mg/mL BrdU immediately following surgery. After one week, we sacrificed 3 mice for analysis. Partial hepatectomy (PHx), in which two-thirds of the liver of a mouse is removed, was then performed on 5 of the 11 mice and the remaining 3 mice were used for controls. One week later, all 8 mice were sacrificed for analysis. Using histological sections, we determined the amount of hepatocyte engraftment in the LN by counting GFP[+] hepatocytes and determined the ratio of proliferating hepatocytes by counting BrdU[+] hepatocytes.

Allogeneic transplantation

Primary hepatocytes from C57BL/6 GFP[+] mice were transplanted into ten 129sv Fah^{−/−} mice by LN or splenic injection. Five out of ten mice from each group were intraperitoneally injected with the immunosuppressive drugs CTLA1Ig (0.25mg) and MR1 (0.25mg), a kind gift from Dr. Fadi Lakkis (University of Pittsburgh), on day 0, 2, 4 and 6 after transplantation.

Antibodies

Antibodies specific for the following antigens were purchased for immunohistochemistry: ER-TR7, LYVE1, GFP, Glutamine Synthetase, CCR7, S1PR1 (EDG1), F4/80 (Abcam), PNAd, B220, CD4 CD8 and Gr-1 (BD Biosciences), BrdU (Santa Cruz biotechnology), DPPIV (AbD Serotec), E-Cadherin (Zymed), Keratin 5 (Covance), Keratin 8 (DSHB), and C-peptide and Glucagon (Cell Signaling Technologies). Antibodies specific for the following antigens were purchased for flow cytometric analysis: APC mouse-CD3ε, APC-Cy7 mouse-CD8α, PE-Cy7-mouse CD45, PE mouse-CD4, mouse Vβ TCR screening panel, mouse naïve/memory T cell panel (Pharmingen), and mouse Treg detection kit (Miltenyi). Appropriate isotype control antibodies (BD Biosciences) were used to estimate background fluorescence.

Immunohistochemistry

Tissue was fixed in 4% paraformaldehyde for 4 hours, stored in 30% sucrose for 12 hours and then embedded in OCT medium, frozen, and stored at −80° C. Sections (5–10μm) were mounted on glass slides and fixed in cold acetone for 10 minutes. For IHC staining, sections were washed with PBS and blocked with 5% BSA or milk for 30 minutes. Sections were then incubated with primary antibody for 1 hour and secondary antibody for 30 minutes. Sections were mounted with Hoechst mounting media. Images were captured with an Olympus FluoView 1000 Confocal Microscope or an Olympus IX71 inverted microscope.

Flow Cytometry

Whole blood was collected in K_2EDTA collection tubes (Terumo Medical). One hundred microliters of blood was added to cold FACS tubes. Antibodies were added at a dilution of 1/10 in blood and mixed by gentle pipetting. Reactions were incubated in the dark in an ice-slurry bath for 30 minutes. Three mL of Red Blood Cell Lysing Buffer (Sigma) was added to each tube, lightly vortexed and incubated for an additional 5 minutes. Two mL of flow buffer (2% FBS in HBSS) was added to the tubes, mixed, and centrifuged at 500g for 5 minutes. The supernatant was aspirated and secondary antibody was added at a dilution of 1/50 in flow buffer and mixed by gentle pipetting. Reactions were incubated in the dark in an ice-slurry bath for 15 minutes. Red blood cell lysis and centrifuge were repeated as described. Final cell pellet was resuspended in 400 μl of flow buffer with propidium iodide. Cells were analyzed using the BD FACSVantage Cell Sorter, a BD Aria II Cell Sorter, or a Miltenyi MACSQuant.

Tail Skin Graft

Recipient mice (BALB/c Nude) containing an ectopic thymus (C57BL/6) in the LN were anesthetized and the tail skin (5×5mm) from CBA/CaJ or C57BL/6 mice was grafted on the left and right lateral sides of the superior dorsal region of the recipient mouse, respectively. A bandage was applied and removed 7 days following surgery. The grafts were observed daily for rejection.

Tumor Cell Transplantation

Human metastatic colon cancer cells (Tu#12) were prepared and transplanted into mice as previously described[33]. Briefly, 3×10^5 cells were transplanted by subcutaneous injections. Tumor size was recorded after 2 months.

LPS induced inflammation

LPS (1 mg/kg, Sigma) was injected intraperitoneally into C57BL/6 wild type or normoglycemic mice that previously received an islet transplant to the LN. Mice were bled to determine glucose levels or to measure serum cytokine levels. Cytokine level was determined by ELISA assay for TNF, IL-1β, and IL-6 (eBioscience).

Statistical Analysis

Statistical significance was determined with an unpaired two-tailed Student's t-test for data in Fig 1e, 2d, 3a.

Supplementary Material

Refer to Web version on PubMed Central for supplementary material.

Acknowledgments

References

1. Fisher RA, Strom SC. Human hepatocyte transplantation: worldwide results. Transplantation. 2006; 82:441–449. [PubMed: 16926585]

2. Shapiro AM, et al. International trial of the Edmonton protocol for islet transplantation. N Engl J Med. 2006; 355:1318–1330. [PubMed: 17005949]

3. Schuppan D, Afdhal NH. Liver cirrhosis. Lancet. 2008; 371:838–851. [PubMed: 18328931]

4. Markert ML, et al. Transplantation of thymus tissue in complete DiGeorge syndrome. N Engl J Med. 1999; 341:1180–1189. [PubMed: 10523153]

5. Markert ML, Devlin BH, McCarthy EA. Thymus transplantation. Clin Immunol. 2010; 135:236–246. [PubMed: 20236866]

6. Merani S, Toso C, Emamaullee J, Shapiro AM. Optimal implantation site for pancreaticislet transplantation. Br J Surg. 2008; 95:1449–1461. [PubMed: 18991254]

7. Dhawan A, Puppi J, Hughes RD, Mitry RR. Human hepatocyte transplantation: current experience and future challenges. Nat Rev Gastroenterol Hepatol. 2010; 7:288–298. [PubMed: 20368738]

8. Cyster JG. Chemokines and cell migration in secondary lymphoid organs. Science. 1999; 286:2098–2102. [PubMed: 10617422]

9. von Andrian UH, Mempel TR. Homing and cellular traffic in lymph nodes. Nat Rev Immunol. 2003; 3:867–878. [PubMed: 14668803]

10. Sleeman JP, Thiele W. Tumor metastasis and the lymphatic vasculature. Int J Cancer. 2009; 125:2747–2756. [PubMed: 19569051]

11. Link A, et al. Fibroblastic reticular cells in lymph nodes regulate the homeostasis of naive T cells. Nat Immunol. 2007; 8:1255–1265. [PubMed: 17893676]

12. Robertson RP. Islet transplantation as a treatment for diabetes - a work in progress. N Engl J Med. 2004; 350:694–705. [PubMed: 14960745]

13. Hoppo T, Komori J, Manohar R, Stolz DB, Lagasse E. Rescue of lethal hepatic failure by hepatized lymph nodes in mice. Gastroenterology. 2011; 140:656–666. e652. [PubMed: 21070777]

14. Van den Broeck W, Derore A, Simoens P. Anatomy and nomenclature of murine lymph nodes: Descriptive study and nomenclatory standardization in BALB/cAnNCrl mice. J Immunol Methods. 2006; 312:12–19. [PubMed: 16624319]

15. Perl AK, Wilgenbus P, Dahl U, Semb H, Christofori G. A causal role for E-cadherin in the transition from adenoma to carcinoma. Nature. 1998; 392:190–193. [PubMed: 9515965]

16. Pham TH, et al. Lymphatic endothelial cell sphingosine kinase activity is required for lymphocyte egress and lymphatic patterning. The Journal of experimental medicine. 2010; 207:17–27. [PubMed: 20026661]

17. Grigorova IL, et al. Cortical sinus probing, S1P1-dependent entry and flow-based capture of egressing T cells. Nature immunology. 2009; 10:58–65. [PubMed: 19060900]

18. Shields JD, et al. Autologous chemotaxis as a mechanism of tumor cell homing to lymphatics via interstitial flow and autocrine CCR7 signaling. Cancer cell. 2007; 11:526–538. [PubMed: 17560334]

19. Michalopoulos GK, DeFrances MC. Liver regeneration. Science. 1997; 276:60–66. [PubMed: 9082986]

20. Grompe M, et al. Pharmacological correction of neonatal lethal hepatic dysfunction in a murine model of hereditary tyrosinaemia type I. Nat Genet. 1995; 10:453–460. [PubMed: 7545495]

21. Overturf K, al-Dhalimy M, Ou CN, Finegold M, Grompe M. Serial transplantation reveals the stem-cell-like regenerative potential of adult mouse hepatocytes. The American journal of pathology. 1997; 151:1273–1280. [PubMed: 9358753]

22. Lagasse E, et al. Purified hematopoietic stem cells can differentiate into hepatocytes in vivo. Nat Med. 2000; 6:1229–1234. [PubMed: 11062533]

23. Notenboom RG, de Boer PA, Moorman AF, Lamers WH. The establishment of the hepatic architecture is a prerequisite for the development of a lobular pattern of gene expression. Development. 1996; 122:321–332. [PubMed: 8565845]

24. Katakai T, Hara T, Sugai M, Gonda H, Shimizu A. Lymph node fibroblastic reticular cells construct the stromal reticulum via contact with lymphocytes. J Exp Med. 2004; 200:783–795. [PubMed: 15381731]

25. Gretz JE, Anderson AO, Shaw S. Cords, channels, corridors and conduits: critical architectural elements facilitating cell interactions in the lymph node cortex. Immunol Rev. 1997; 156:11–24. [PubMed: 9176696]

26. Lakkis FG, Arakelov A, Konieczny BT, Inoue Y. Immunologic 'ignorance' of vascularized organ transplants in the absence of secondary lymphoid tissue. Nature medicine. 2000; 6:686–688.

27. Siegler EL, Tick N, Teresky AK, Rosenstraus M, Levine AJ. Teratocarcinoma Transplantation Rejection Loci: An H-2-Linked Tumor Rejection Locus. Immunogenetics. 1979; 9:207–220.

28. Dressel R, et al. The tumorigenicity of mouse embryonic stem cells and in vitro differentiated neuronal cells is controlled by the recipients' immune response. PloS one. 2008; 3:e2622. [PubMed: 18612432]

29. Bumgardner GL, Li J, Heininger M, Orosz CG. Costimulation pathways in host immune responses to allogeneic hepatocytes. Transplantation. 1998; 66:1841–1845. [PubMed: 9884287]

30. Gao D, Li J, Orosz CG, Bumgardner GL. Different costimulation signals used by CD4(+) and CD8(+) cells that independently initiate rejection of allogenic hepatocytes in mice. Hepatology (Baltimore, Md). 2000; 32:1018–1028.

31. Rodewald HR. Thymus organogenesis. Annu Rev Immunol. 2008; 26:355–388. [PubMed: 18304000]

32. Pearse G. Normal structure, function and histology of the thymus. Toxicol Pathol. 2006; 34:504–514. [PubMed: 17067941]

33. Odoux C, et al. A stochastic model for cancer stem cell origin in metastatic colon cancer. Cancer Res. 2008; 68:6932–6941. [PubMed: 18757407]

34. Ohashi K, et al. Liver tissue engineering at extrahepatic sites in mice as a potential new therapy for genetic liver diseases. Hepatology. 2005; 41:132–140. [PubMed: 15619229]

35. Rodeck B, Kardorff R, Melter M, Schlitt HJ, Oldhafer KJ. Auxiliary partial orthotopic liver transplantation for acute liver failure in two children. Pediatric transplantation. 1999; 3:328–332. [PubMed: 10562979]

36. Sanz-Rodriguez F, et al. Endoglin regulates cytoskeletal organization through binding to ZRP-1, a member of the Lim family of proteins. J Biol Chem. 2004; 279:32858–32868. [PubMed: 15148318]

37. Gerber SA, et al. Preferential attachment of peritoneal tumor metastases to omental immune aggregates and possible role of a unique vascular microenvironment in metastatic survival and growth. The American journal of pathology. 2006; 169:1739–1752. [PubMed: 17071597]

38. Lawenda BD, Mondry TE, Johnstone PA. Lymphedema: a primer on the identification and management of a chronic condition in oncologic treatment. CA Cancer J Clin. 2009; 59:8–24. [PubMed: 19147865]

39. Senti G, et al. Intralymphatic allergen administration renders specific immunotherapy faster and safer: a randomized controlled trial. Proc Natl Acad Sci U S A. 2008; 105:17908–17912. [PubMed: 19001265]

40. Kim M, et al. Ultrasound-guided mesenteric lymph node iohexol injection for thoracic duct computed tomographic lymphography in cats. Vet Radiol Ultrasound. 2011; 52:302–305. [PubMed: 21554478]

41. Gordon RD, Starzl TE. Changing perspectives on liver transplantation in 1988. Clinical transplants. 1988:5–27. [PubMed: 3154494]

42. Stampfl DA, et al. Heterotopic liver transplantation for fulminant Wilson's disease. Gastroenterology. 1990; 99:1834–1836. [PubMed: 2227300]

43. Rice HE, et al. Thymic transplantation for complete DiGeorge syndrome: medical and surgical considerations. J Pediatr Surg. 2004; 39:1607–1615. [PubMed: 15547821]

44. Jiang J, Wang H, Madrenas J, Zhong R. Surgical technique for vascularized thymus transplantation in mice. Microsurgery. 1999; 19:56–60. [PubMed: 10188826]

45. Harlan DM, Kenyon NS, Korsgren O, Roep BO. Current advances and travails in islet transplantation. Diabetes. 2009; 58:2175–2184. [PubMed: 19794074]

46. Fiorina P, Shapiro AM, Ricordi C, Secchi A. The clinical impact of islet transplantation. Am J Transplant. 2008; 8:1990–1997. [PubMed: 18828765]

47. Takahashi K, Yamanaka S. Induction of pluripotent stem cells from mouse embryonic and adult fibroblast cultures by defined factors. Cell. 2006; 126:663–676. [PubMed: 16904174]

48. Zhao T, Zhang ZN, Rong Z, Xu Y. Immunogenicity of induced pluripotent stem cells. Nature. 2011; 474:212–215. [PubMed: 21572395]
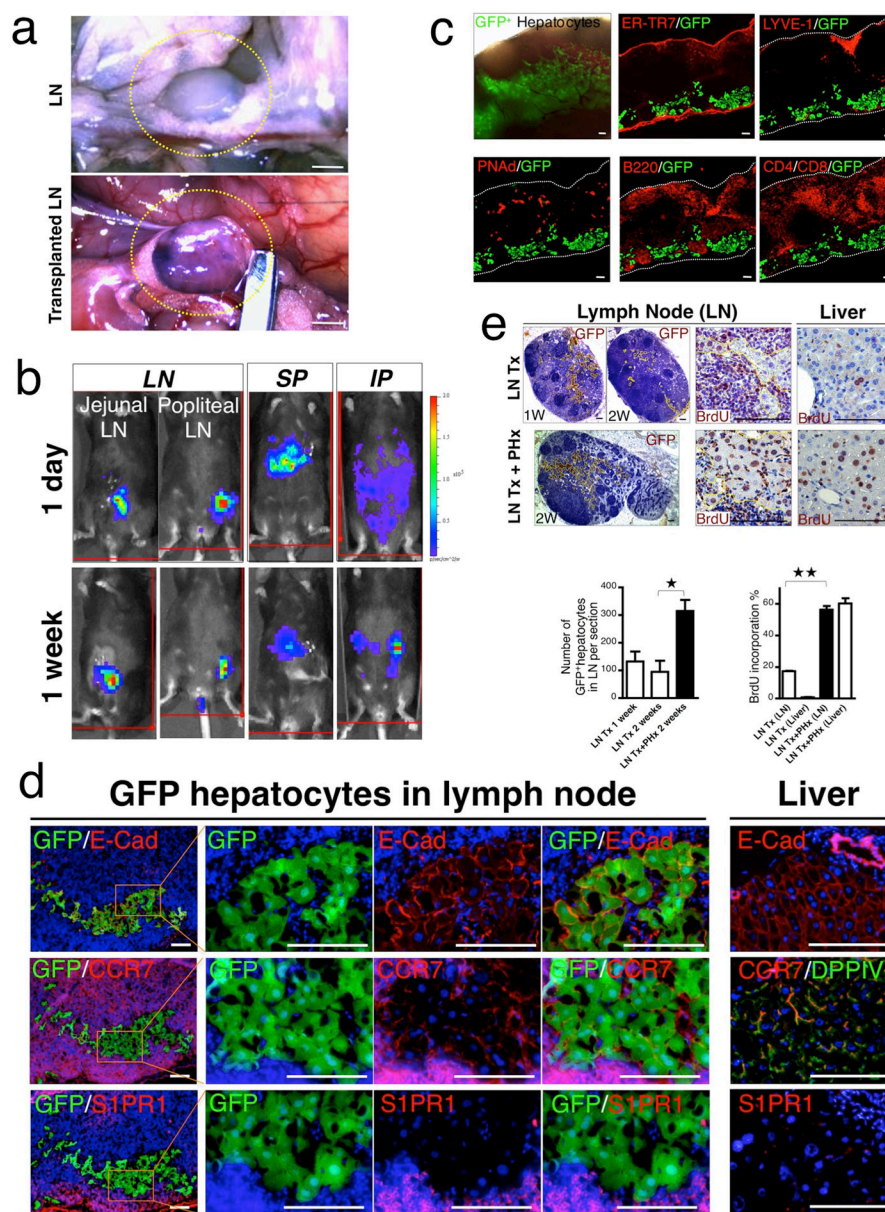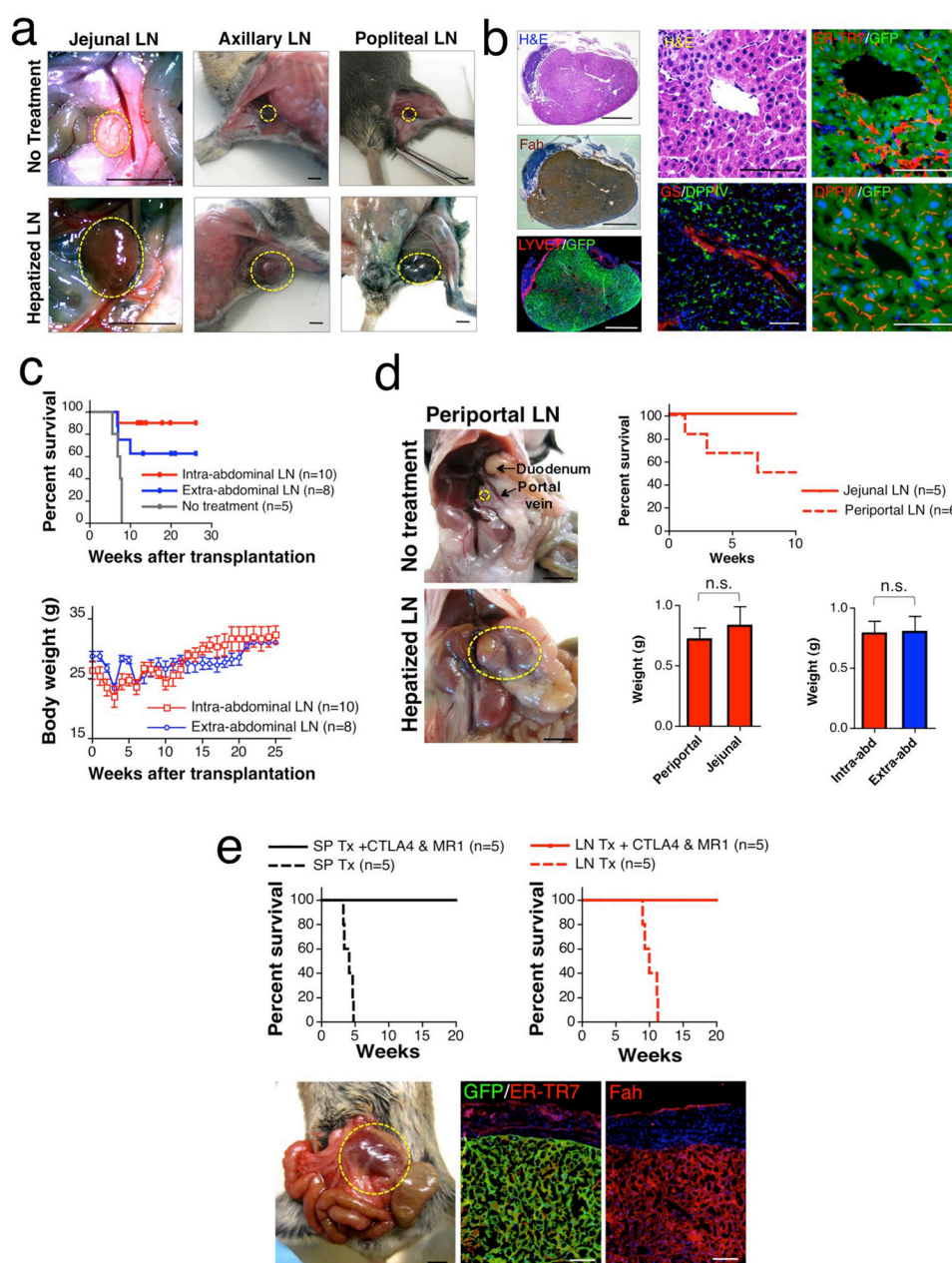
Figure 1.

Direct injection of hepatocytes into a single lymph node (LN) of a C57BL/6 wild type mouse. (**a**) Jejunal LN (yellow dotted oval) not transplanted (top panel) and just after transplantation (bottom panel) with hepatocytes. Primary hepatocytes were mixed with 3% Evans blue dye and Matrigel before injection. (**b**) *In vivo* optical imaging of animals transplanted at different sites. Primary hepatocytes from luciferase transgenic mice were transplanted in a single jejunal or popliteal LN, in spleen (SP) or intraperitoneally (IP). Signals (blue to red) depict different concentrations of donor hepatocytes at day 1 (top panels) and 1 week (bottom panels) after transplant. (**c**) Distribution of donor hepatocytes in a single jejunal LN. Top left panel, whole mount imaging of a LN one week after injection of donor GFP⁺ hepatocytes. Bright field was merged with fluorescence. Top middle to

bottom right panels, immunofluorescent (IF) staining of frozen LN serial sections with mAbs (red) against ER-TR7 (reticular fibroblasts), LYVE-1 (lymphatic vessels), PNAd (high endothelial venules), B220 (B cells) and CD4/CD8 (CD4 T and CD8 T cells) with the presence of GFP[+] hepatocytes (green). (**d**) IF staining of donor GFP+ hepatocytes (green) in jejunal LN one week after transplantation. Serial sections were stained with mAbs (red) against E-Cadherin (ECad), C-C chemokine receptor type 7 (CCR7) and sphingosine-1-phosphate receptor 1 (S1PR1). Nativel iver sections were stained as control (right panels). In native liver, CCR7 (red) was co-stained with dipeptidyl peptidase-4 (DPPIV) (green). All sections were counterstained with Hoechst 33342 (blue). (**e**) Proliferation of engrafted hepatocytes in LN after partial hepatectomy (PHx). Paraffin sections of injected LN and corresponding native liver one and two weeks after transplantation. Sections were stained for GFP (one and two weeks after transplantation) and BrdU (two weeks after transplantation), and revealed by peroxidase (brown cytoplasmic and brown nuclei staining respectively). Sections were counterstained with hematoxylin. Yellow outlines mark small populations of GFP[+] hepatocytes. 2 weeks after transplantation, bar graphs show the number of GFP[+] hepatocytes and % of BrdU[+] hepatocytes observed per section after immunostaining from animals with or without PHx.* $P<0.05$, ** $P<0.0001$. Data (mean + sem) are representative of one experiment with three to five mice per group. The experiment was repeated two times. Scale bar: (a) 1mm, (c–e) 100μm.

Figure 2.

Direct injection of hepatocytes into a single LN of a Fah$^{-/-}$ mouse. (**a**) Macroscopic appearances of non-transplanted and transplanted (hepatized) LN; LN are marked by yellow dotted oval). For non-transplanted axillary and popliteal LN, Evans blue was injected to highlight the presence of the LN.. The representative images of the jejunal, axillary and popliteal hepatized LN were captured at 12, 22, 25 weeks after transplantation respectively. (**b**) Histology of hepatized jejunal LN in rescued Fah$^{-/-}$mice. Left panels, serial sections of hepatized LN composed of hepatic and lymphatic tissue. Sections are stained with hematoxylin and eosin (H&E)(top left panel), Fah (brown) and counterstained with hematoxylin (blue)(middle left panel). The immunofluorescence shows lymphatic vessels

(LYVE1, red) and hepatocytes (GFP$^+$, green)(bottom left panel). Right panels, higher magnification of H&E showing typical cuboidal hepatocytes. Reticular fibroblasts stain with antibodies specific for ER-TR7 (red) while hepatocytes are GFP$^+$, and stain with antibodies specific for DPPIV (red). Glutamine synthetase (GS, red) expression shows unique zonal restriction surrounding terminal hepatic venules. Sections were counterstained with Hoechst 33342 (blue). (**c**) Kaplan-Meier survival curves (top) and body weight (bottom) of Fah$^{-/-}$ mice transplanted in intra- and extra- (blue) abdominal LN vs no treatment. Error bars show standard error. (**d**) Comparison of transplant efficiency in different sites. Left panels, macroscopic appearances of normal and hepatized LN (yellow dotted ovals) in the periportal area. Right top panel, Kaplan-Meier survival curves of Fah$^{-/-}$ mice transplanted into the jejunal vs periportal LN. Right lower panels, average weight of periportal vs jejunal LN and intra- vs extra- abdominal LN. No statistical difference was observed. Error bars show s.e.m. (**e**) Top panels, allogeneic transplantation in LN (LN Tx) and splenic injection (SP Tx). GFP$^+$ hepatocytes (C57BL/6 background) were transplanted into Fah$^{-/-}$ mice (129 sv background) by SP Tx and LN Tx and after NTBC removal (lack of NTBC in drinking water induces liver failure in Fah$^{-/-}$ mice). Where indicated, mice were injected with immunosuppressive agents CTLA4-Ig and MR1 on day 0, 2, 4 and 6 after transplantation. The experiment was repeated at least 2 times. Lower panels show one representative LN Tx mouse injected with CTLA4-Ig and MR1. Macroscopic appearance of hepatized jejunal LN (yellow dotted oval). Immunostaining of the hepatized LN for the presence of GFP+ (green) and Fah+ (red) hepatocytes as well as reticular fibroblasts (ER-TR7, red). Sections were counterstained with Hoechst 33342 (blue). Scale bar: (a, d and e, left panels) 5mm, (b, left panels) 1mm and (b, middle right and e middle right panels) 100μm.
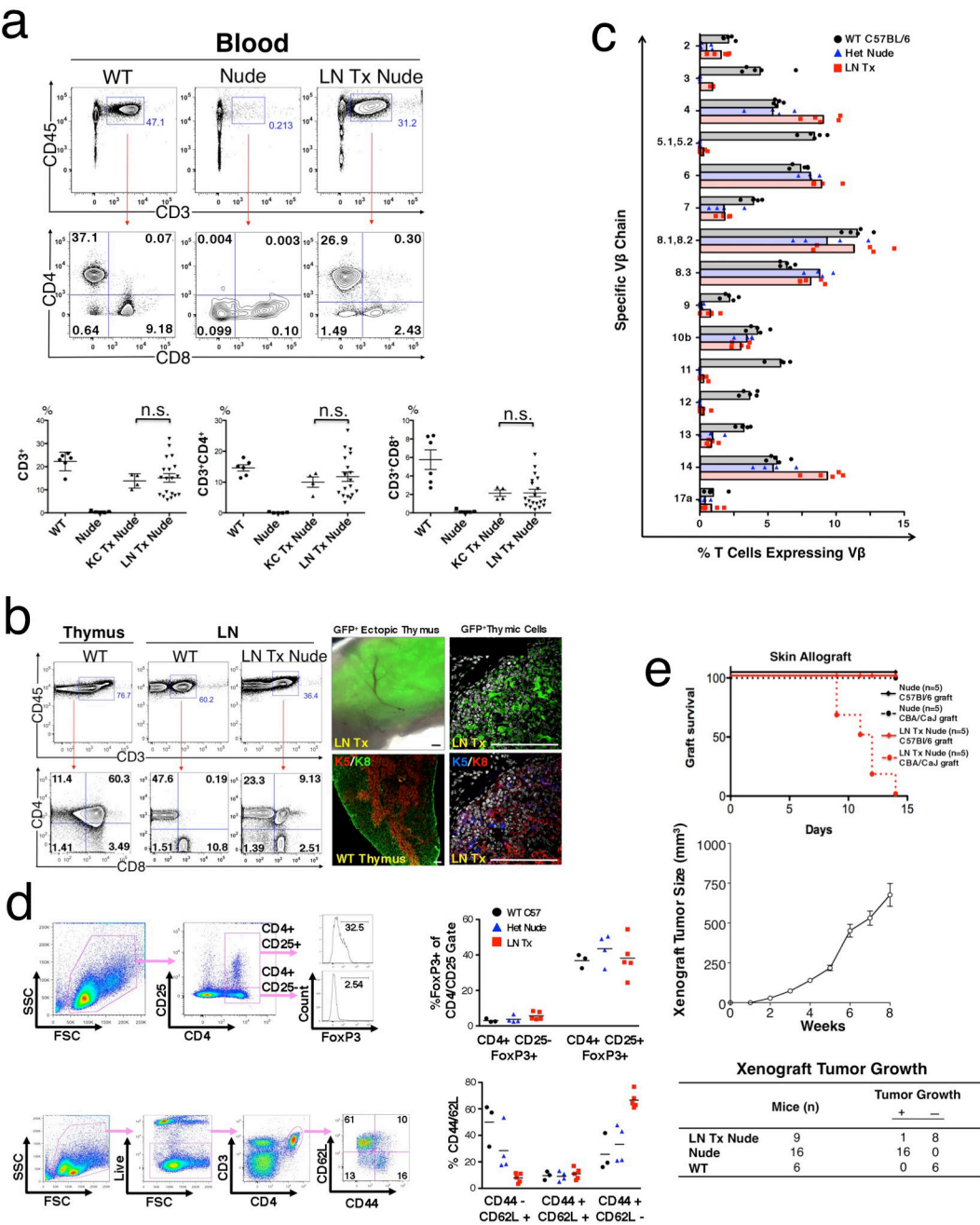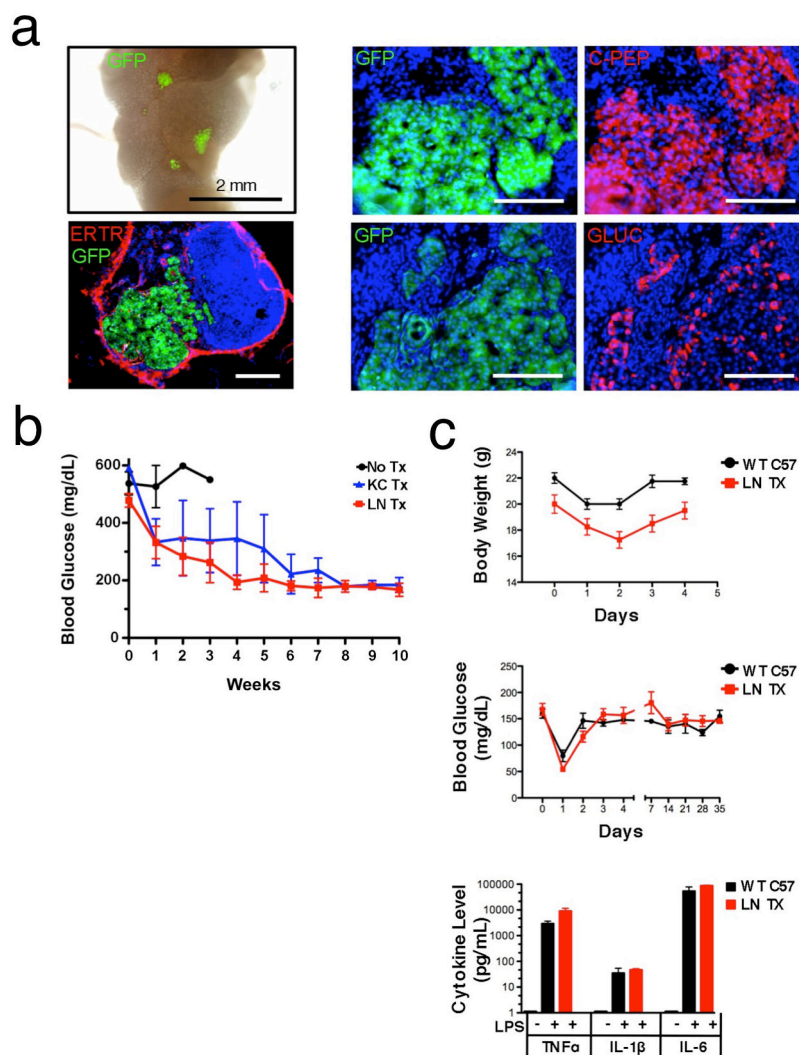
Figure 3.
Functional ectopic thymus in the jejunal LN. (**a**) Flow cytometric analysis of peripheral blood T cells. Top panels, representative analysis of the gating strategy for CD4 and CD8 T cells in wild type C57BL/6 (WT), BALB/c Nude (Nude), and BALB/c Nude mice into which C57BL/6 GFP+ thymic cells were injected into a jejunal LN (LN Tx Nude) mice. The number values assigned to the gates and quadrants represent the percentage of total live cells within that gate or quadrant. All contour plots display 10% probability contours. Lower panels show the percentage of CD3+, CD3+CD4+ and CD3+CD8+ live T cells in the blood of each animal analyzed (each symbol represents one animal); animals were WT, Nude, KC

Tx Nude (BALB/c Nude Transplanted under Kidney Capsule) and LN Tx Nude. The thin black line indicates the mean +/− sem. No statistical significance (n.s.) was observed between KC and LN transplantation in each of the 3 panels. (**b**) Left panels, representative flow cytometric analysis of cells present in wild type C57BL/6 (WT) thymus and LN, and LN of BALB/c Nude mice into which thymic cells were injected into the LN (LN Tx Nude). The number values assigned to the gates and quadrants represent the percentage of total live cells within that gate or quadrant. Right panels show (top left) whole mount jejunal LN of a Nude mouse engrafted in LN with GFP+ thymic cells. Bright field was merged with fluorescence, Top right shows frozen section with GFP+ donor thymic cells. Bottom right shows immunostaining of cytokeratin 5 (K5) (blue), cytokeratin 8 (K8) (red) and counterstaining with Hoechst (white). Bottom left shows WT native thymus stained for K5 (red) and K8 (green). Scale bar: 200μm. (**c**) Flow cytometric analysis of TCR Vβ segment expression in splenocytes from wild type C57BL/6 mice (WT C57BL/6), heterozygous BALB/c Nude mice (Het Nude), or LN transplanted BALB/c Nude mice (LN Tx). Bar graphs show the mean percentage of the particular Vβ receptor. Individual symbols represent data from a single mouse (n=4–5). (**d**) Flow cytometric analysis of regulatory, naïve, central memory, and effector memory T cell subsets in splenocytes. Dot plots and histograms show gating strategy to detect regulatory T cells (FoxP3+ fraction of CD4+CD25+ T cells) and naïve (CD44−CD62L+), central memory (CD44+CD62L+), and effector memory (CD44+CD62L−) T cells. Graphs show the data from individual mice, labeled as in panel **c**. The thin black line indicates the mean. (**e**) Top panel, Kaplan-Meier curves showing survival of skin grafts from C57BL/6 or CBA/CaJ donor mice transplanted onto BALB/c Nude recipients that had previously undergone transplantation of C57BL/6 thymic cells into the LN. Middle panel, graph of tumor growth in athymic BALB/c Nude (nu/nu) mice. 300,000 human colon cancer cells[33] were inoculated subcutaneously with matrigel. Tumor sizes were measured once per week using a caliper and calculated as $(\pi/6) \times$ (length (mm) $\times$ width^2 (mm^2)). The experiment was terminated after 8 weeks. Values are mean +/− s.e.m., n=10. Bottom panel, presence (+) or absence (−) of tumor growth after a single subcutaneous injection of 300,000 human colorectal cancer cells into BALB/c Nude recipients that had previously undergone transplantation of C57BL/6 thymic cells into the LN (LN Tx Nude), BALB/c Nude (Nude) recipients or C57BL/6 wild-type (WT) recipients.

Figure 4.
Ectopic pancreas generation in the jejunal LN after islet transplantation. (**a**) Top panel shows whole mount LN of a streptozotocin-treated diabetic C57BL/6 mouse engrafted with C57BL/6 GFP$^+$ pancreatic islets. Bright field was merged with fluorescence. Other panels show immunofluorescence (IF) of LN removed 6 weeks after engraftment. Staining with antibodies specific for ERTR7 (reticular fibroblasts), C-peptide (C-PEP), and glucagon (GLUC) is shown in red and GFP is shown in green and Hoechst counterstain is shown in blue. (**b**) Average blood glucose levels in diabetic recipient mice over the course of 10 weeks after transplantation of islets into the jejunal LN (LN Tx, n=5), under the kidney capsule (KC Tx, n=3), and without transplantation (No Tx, n=6). In 3 of 5 LN Tx mice, a second islet transplant was performed into the jejunal LN one week after the initial transplant. The mice that did not receive a transplant all died after 3 weeks. The data are presented as mean +/− s.e.m. (**c**) Average body weight (top) and blood glucose level (middle) of C57BL/6 wild-type (WT) mice or C57BL/6 LN Tx mice after LPS injection (1 mg/kg). Bottom panel shows average serum concentrations of tumor necrosis factor alpha

(TNFα), IL1-β, and IL-6 two hours after LPS injection. All error bars show standard error. All IF image scale bars are 100 μm unless otherwise indicated.
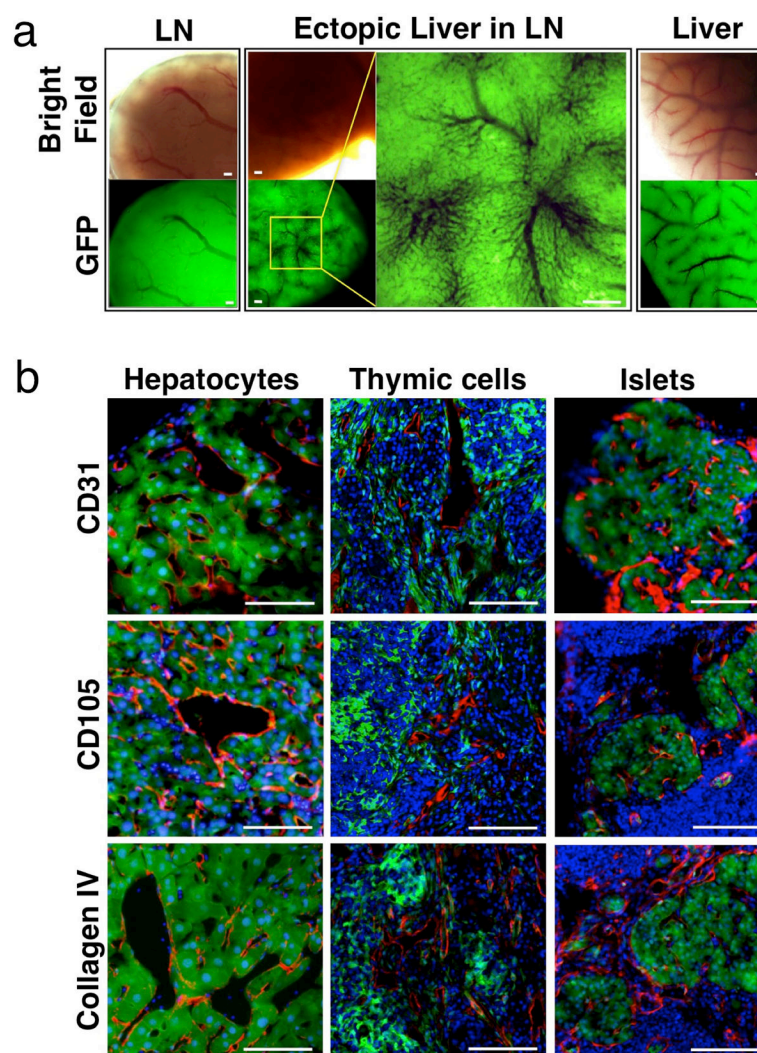
Figure 5.
Neo-vascularization of ectopic tissue. (**a**) Vascular trees are shown in a native LN and native liver of a GFP transgenic mouse, and in mice after hepatocyte transplantation into the LN. (**b**) Immunostaining of LN injected with hepatocytes, thymic cells and pancreatic islets. Images were captured 12, 15, and 6 weeks after transplant of each tissue, respectively. CD31 is a marker for blood vessels and CD105 and Collagen IV are markers for neo-vascularization. Vasculature markers are shown in red and ectopic tissue is shown in green. All sections were counterstained with Hoechst 33342 in blue. All scale bars are 100μm.